Meteorological Events Affecting Cold-Air Pools in a Small Basin

MANFRED DORNINGER

Department of Meteorology and Geophysics, University of Vienna, Vienna, Austria

C. DAVID WHITEMAN

Department of Atmospheric Sciences, University of Utah, Salt Lake City, Utah

BENEDIKT BICA,* STEFAN EISENBACH, BERNHARD POSPICHAL, AND REINHOLD STEINACKER

Department of Meteorology and Geophysics, University of Vienna, Vienna, Austria

(Manuscript received 15 October 2010, in final form 31 May 2011)

ABSTRACT

Meteorological events affecting the evolution of temperature inversions or cold-air pools in the 1-km-diameter, high-altitude (~1300 m MSL) Grünloch basin in the eastern Alps are investigated using data from lines of temperature dataloggers running up the basin sidewalls, nearby weather stations, and weather charts. Nighttime cold-air-pool events observed from October 2001 to June 2002 are categorized into undisturbed inversion evolution, late buildups, early breakups, mixing events, layered erosion at the inversion top, temperature disturbances occurring in the lower or upper elevations of the pool, and inversion buildup caused by the temporary clearing of clouds. In addition, persistent multiday cold-air pools are sometimes seen. Analyses show that strong winds and cloud cover are the governing meteorological parameters that cause the inversion behavior to deviate from its undisturbed state, but wind direction can also play an important role in the life cycle of the cold-air pools, because it governs the interaction with steep or gentle slopes of the underlying topography. Undisturbed cold-air pools are unusual in the Grünloch basin. A schematic diagram illustrates the different types of cold-air-pool events.

1. Introduction

Life cycles (formation, maintenance, and breakup) of cold-air pools in sinkholes and valleys of different scales have been studied for more than 30 years. The majority of these (semi-) analytical and numerical modeling studies focused on the processes responsible for cold-air-pool breakup. Among these are dissipation of the cold-air pool by convective boundary layer growth after sunrise (Whiteman and McKee 1982), convective boundary layer growth due to heated sidewalls and subsidence of the stable cold-air core (Whiteman et al. 2004c), cold-air advection aloft (Zhong et al. 2001), turbulent erosion at the top of the cold-air pool (Petkovšek 1992; Vrhovec and Hrabar 1996; Rakovec et al. 2002; Zhong et al. 2003; Fritts et al. 2010), air drainage from valleys (Zängl 2002), and the passage of fronts (Whiteman et al. 2001).

Relatively few studies have examined the formation and maintenance of cold-air pools. Whiteman et al. (2001) investigated two persistent cold-air-pool events in the Columbia basin, which were also simulated using a mesoscale numerical model (Zhong et al. 2001). Billings et al. (2006) used a numerical model to simulate the maintenance of the valley cold pool in the upper Yampa Valley of northwestern Colorado. The formation of extreme cold-air pools was studied by Zängl (2005) in elevated sinkholes using an idealized numerical model. Yao and Zhong (2009) used data from the Meteor Crater Experiment (METCRAX; Whiteman et al. 2008) to analyze the formation and destruction of a temperature inversion in the crater. A comprehensive review of the existing literature can be found in, for example, Whiteman (1990), Clements et al. (2003), and Steinacker et al. (2007).

* Current affiliation: Central Institute for Meteorology and Geodynamics, Vienna, Austria.

Corresponding author address: C. David Whiteman, Dept. of Atmospheric Sciences, 135 S 1460 E, Rm. 819, Salt Lake City, UT 84112-0110.
E-mail: dave.whiteman@utah.edu

DOI: 10.1175/2011JAMC2681.1

Surprisingly few studies have investigated the role of ambient atmospheric conditions on inversion structure and evolution. Whiteman et al. (2001) characterized cold pools as *diurnal*, forming during the evening and decaying following sunrise the next day, or as *persistent*, lasting longer than one night. Their study investigated two cold-pool episodes and used the synoptic background fields to describe the different mechanisms responsible for their initiation and decay. Yao and Zhong (2009) stratified data from the METCRAX field program according to temperature inversion strength and defined three different regimes. In the *fully decoupled* regime the crater atmosphere was completely decoupled from the ambient atmosphere and a strong temperature inversion formed in the undisturbed basin. In contrast, little or no temperature inversion was observed during the *coupled* regime. The *partially decoupled* regime lies between these two regimes. The basin atmosphere could make a transition between the coupled and decoupled regimes during a single night. Most of the existing studies suffer from the relatively short and sparse observational datasets that have been available up to now. This situation has arisen partly because of the relatively harsh environments encountered in high-altitude basins and valleys and the frequent occurrence of low winter-season temperatures. As a result there have been no comprehensive datasets relating long-term measurements of temperature inversions with ambient atmospheric conditions. It is the main purpose of this paper to close this gap.

A meteorological field experiment was conducted in the Grünloch sinkhole or *doline* during the period from 17 October 2001 through 4 June 2002 at an altitude of about 1300 m MSL on the Hetzkogel Plateau in the eastern Alps near Lunz, Lower Austria. This sinkhole, formerly known as the ''Gstettneralm sinkhole'' or ''Gstettnerboden,'' develops strong temperature inversions on clear undisturbed nights and records the lowest minimum temperatures in central Europe. Minimum temperatures in the 150-m-deep sinkhole have fallen as low as −52.6°C (Aigner 1952; Geiger 1965). The purpose of the experiments was to investigate minimum temperatures and cold-air pools that form in this topography (see also Pospichal 2004).

Steinacker et al. (2007) summarized the history of meteorological measurements in the Grünloch sinkhole, the experimental design, the sinkhole topographical characteristics and climate, the measurement program, the meteorological instruments, instrument accuracies, times of operation, locations of measurement sites, snow depths throughout the winter, and other features of this experiment.

As part of the Grünloch meteorological experiment, temperature dataloggers of a type used previously in meteorological research (Whiteman et al. 2000) were installed on wooden posts on three lines that ran up the sidewalls of the *doline* and were operated from 17 October 2001 through 4 June 2002. In early June 2002 a series of tethered balloon soundings were made in the Grünloch over two days and nights. A comparison of tethersonde temperature profiles with ''pseudo-vertical temperature profiles'' from the lines of temperature loggers showed that the logger lines provided good proxy soundings of the free atmosphere in the sinkhole under stable nighttime conditions with low background winds (Whiteman et al. 2004a). They found a standard deviation of 0.4°C for this case, which increased to 1°–2°C for moderate winds of up to 4 m s^{-1} aloft with gusts of up to 10 m s^{-1}, which is still a fairly good approximation. Because of the fact that temperature profiles from tethersonde launches are available for only two nights, their findings cannot be generalized for all possible weather situations. Nonetheless, we have assumed that the lines of temperature loggers provide a reasonable proxy for free-air temperature profiles on a qualitative basis rather than on a quantitative one for moderate-to-strong winds.

Steinacker et al. (2007) provided in their overview of the Grünloch experiments some examples of the effects of different meteorological events on the basin atmosphere. Following their initial findings, we have examined the entire temperature logger dataset and classified many of the cold-air-pool events that occurred in the sinkhole over the period of record. Individual events were investigated further using data from three weather stations that were operated in the Grünloch and its immediate surroundings and from synoptic weather charts.

In this work, we survey the data from the experiment, develop a classification scheme for the major cold-air-pool events according to the temperature records, classify the events that occurred over the experimental period, and provide explanations of the weather situations leading to these events. Study of these events is expected to increase understanding of the factors that affect the evolution of cold-air pools in confined topography.

A detailed description of the dataset is given in section 2. Section 3 summarizes the main topographical and meteorological parameters that govern the life cycle of the cold-air pool. Section 4 classifies observed cold-air-pool events according to their temperature records and supporting meteorological data. The results are summarized and conclusions are drawn in section 5.

2. The dataset

A map of the Grünloch basin showing the locations of meteorological equipment used in this paper is shown in Fig. 1. The dataset contains 230 days of instantaneous

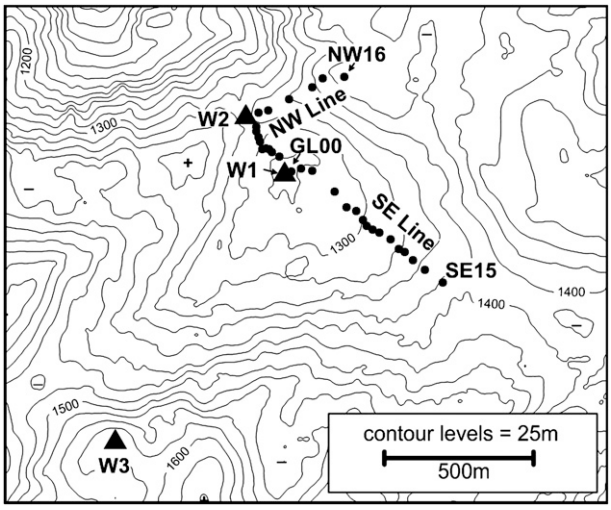

FIG. 1. Topographic map of the Grünloch basin showing the two lines of temperature dataloggers (filled circles) and the three weather stations (triangles): W1 (Grünloch floor), W2 (Lechner Saddle), and W3 (Kleiner Hühnerkogel).

TABLE 1. Temperature datalogger altitudes.

Site	Alt (m MSL)	Site	Alt (m MSL)
Northwest line		Southeast line	
NW01	1275	SE01	1275
NW02	1282	SE02	1280
NW03	1287	SE03	1285
NW04	1294	SE04	1291
NW05	1299	SE05	1296
NW06D	1304	SE06	1300
NW06U	1304	SE07	1305
NW07	1309	SE08	1310
NW08	1315	SE09	1315
NW09	1320	SE10	1320
NW10D	1324	SE11	1325
NW10U	1324	SE12	1331
NW11	1332	SE13	1340
NW12	1337	SE14D	1360
NW13	1350	SE14U	1360
NW14	1370	SE15	1378
NW15	1392	Basin floor	
NW16	1412	GL00D	1270

temperature readings taken at 5-min intervals from temperature sensors placed in solar radiation shields at 1.4- or 2.2-m heights on wooden poles that ran up the northwest and southeast sidewalls of the Grünloch. Poles were generally separated by vertical distances of about 5 m, although the altitude spacing increased to 10, 15, and 20 m at the upper elevations of the sinkhole. The exact altitudes of the sensors are given in Table 1. For further details on sensor locations and accuracies, the reader is referred to Steinacker et al. (2007). The northwest line was on the steepest terrain and is considered to have provided the most representative free-air temperatures within the *doline*. This line also had the highest concentration of dataloggers. In late winter, however, several dataloggers on this line were buried by deep snowfalls (Steinacker et al. 2007) and some of the poles were tipped out of vertical orientation by the slow creep of the snowpack down the steep slopes. Late-winter events are thus illustrated with data from the gentler slopes on the southeast line.

Supporting weather data came from three Vaisala, Inc., automatic weather stations, which were operated with a 1- or 5-min time resolution, one on the sinkhole floor at 1270 m MSL, one 53 m above the floor at the Lechner Saddle (the lowest-altitude outlet from the sinkhole), and one 331 m above the floor at the summit of the Kleiner Hühnerkogel. The heavy midwinter snowpack caused intermittent outages of the automatic weather stations when their solar panels were covered with snow and ice or their sensors were damaged. Nevertheless, the data from the automatic weather stations include temperature, wind speed, and wind direction as well as humidity records for most of the case studies presented in section 4. The accompanying large-scale weather information for each of the selected events was taken from the *Berliner Wetterkarten* of the Institut für Meteorologie der Freien Universität Berlin for 2001 and 2002 (online at http://wkserv.met.fu-berlin.de/) and from the European Centre for Medium-Range Weather Forecasts analyses and is supported by local observations from the nearby synoptic weather stations at Lunz am See (World Meteorological Organization station identifier 11170), Feuerkogel (11155), and Rax Bergstation (11180). Thermal infrared and water vapor satellite images from Meteosat completed the material used for the synoptic descriptions.

3. Some aspects of the formation and breakup of the Grünloch cold-air pool

The strength of temperature inversions and the formation of cold-air pools in sinkholes are determined by topographical and meteorological parameters as well as surface conditions. Whiteman et al. (2004b) studied the effects of different sinkhole geometry for four sinkholes in the Grünloch basin vicinity for snow-free and snow-covered situations. They found that sinkhole drainage area and depth are not the primary topographic factors. Rather, the sky-view factor is the main controlling parameter for the cooling of the basins. The strongest cold-air pools occurred under calm and clear-sky conditions when fresh snow cover was present. For these events, the average inversion strength between the floor of the Grünloch (1270 m MSL) and the Lechnergraben Saddle (1324 m MSL) was 15°–20°C. This temperature difference was

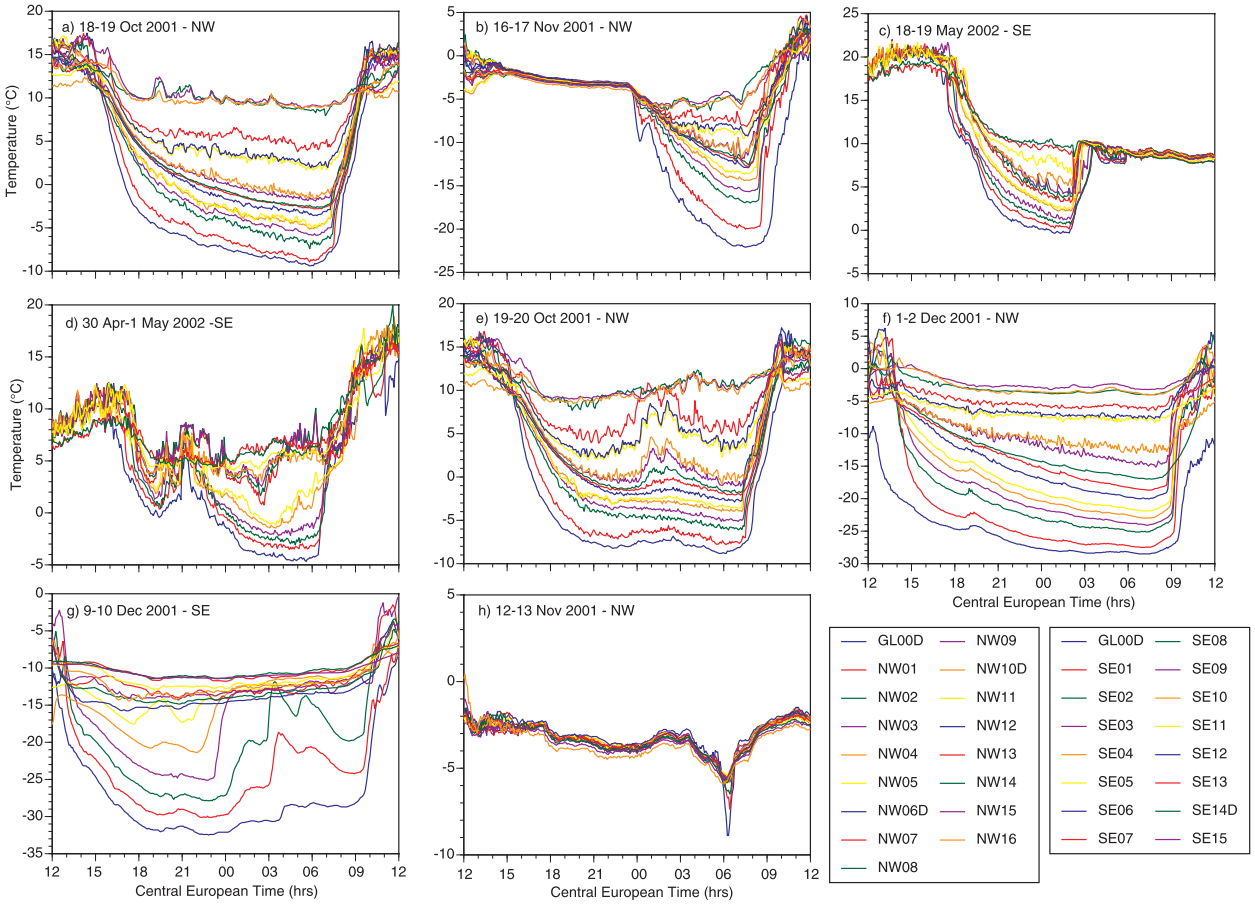

FIG. 2. Examples of cold-air-pool evolution categories using temperature time series from temperature dataloggers at different heights on the northwest or southeast sidewalls of the Grünloch: (a) undisturbed evolution, (b) late buildup, (c) early breakup, (d) mixing event, (e) upper disturbance, (f) lower disturbance, (g) layered erosion, and (h) cold-air-pool window.

typically 5°–10°C for the snow-free case. Even a thin snow cover can increase the strength of the inversion by significantly decreasing the upward heat transfer from the soil. Another critical parameter for cold-air-pool evolution is the moisture content of the prevailing air mass. Whiteman et al. (2007) discussed the effects of dew- and frostfall as well as of fog and cloud formation on the development of the nocturnal inversion. They concluded that latent heat release due to dew-/frostfall may reach 33%–53% of the sensible heat flux loss from the basin for a snow-free basin floor.

Dynamic effects such as turbulent erosion can also play a major role in the destruction of the inversion. The effectiveness of turbulent erosion of the cold-air pool is governed by stability and vertical wind shear as expressed by the ratio of the buoyant production of turbulence to the shear production of turbulence. This dimensionless ratio, the bulk Richardson number R_B, is defined as (e.g., Glickman 2000)

$$R_B = \frac{\dfrac{g}{T_V}\dfrac{\Delta\Theta_V}{\Delta z}}{\left(\dfrac{\Delta u}{\Delta z}\right)^2 + \left(\dfrac{\Delta v}{\Delta z}\right)^2} = \frac{\dfrac{g}{T_V}\Delta\Theta_V \Delta z}{(\Delta u)^2 + (\Delta v)^2},$$

where g is acceleration of gravity, T_V is virtual absolute temperature, Δz is the thickness of the turbulent erosion zone, Δu and Δv are the vertical wind shear components, and $\Delta\Theta_V$ is the vertical virtual potential temperature gradient across this layer, respectively. The critical value for the bulk Richardson number is approximately $R_C = 0.25$ (e.g., Kunze et al. 1990). If $R_B < R_C$, the flow becomes dynamically unstable and turbulent and the cold-air pool will be eroded. The thickness Δz of the turbulent erosion zone was considered to be the upper 10 m of the cold pool. Because continuous tethersonde data were unavailable for the turbulent erosion cases, we could not describe from three weather stations how the erosion layer of 10-m thickness penetrates into the basin. We assumed that the

TABLE 2. Categorization of Grünloch cold-air-pool events by date. The boldface dates are the best examples; the ones in parentheses are marginal.

Category	Description	Dates
1	Undisturbed evolution	**18 Oct**, 3 Nov, 17 Nov, (18 Nov), (30 Nov), (1 Dec), (10 Mar), (12 Mar), 29 Mar, 30 Mar, 31 Mar, (4 Apr), 12 May, **15 May**, **30 May**
2	Late buildup	5 Nov, **16 Nov**, **30 Nov**, 1 Feb, 3 Feb, 17 Feb, 3 Apr, 5 Apr, (10 Apr), 13 Apr, 27 Apr, (14 May), 21 May, 22 May
3	Early breakup	23 Oct, 30 Oct, 31 Oct, 4 Dec, 2 Feb, 9 Feb, (13 Apr), 25 Apr, 26 Apr, (14 May), **18 May**, 27 May
4	Mixing event	17 Oct, 20 Oct, 26 Oct, 27 Oct, 4 Nov, 10 Nov, 13 Dec, 29 Jan, 4 Feb, 5 Feb, 11 Mar, 16 Mar, 17 Mar, (2 Apr), 7 Apr, (10 Apr), 26 Apr, **28 Apr**, **30 Apr**, (11 May), 13 May, (14 May), (16 May)
5	Upper disturbance	19 Oct, 20 Oct, 26 Oct, 31 Oct, 4 Nov, 11 Nov, 15 Nov, 17 Nov, 18 Nov, **2 Dec**, (9 Dec), (14 Dec), (30 Jan), 13 Mar, (14 Mar), (18 Mar), (1 Apr), 4 Apr, 1 May, 6 May, 11 May, 16 May, 17 May
6	Lower disturbance	(19 Oct), **30 Nov**, **1 Dec**, **3 Dec**, **8 Dec**, (9 Dec), (13 Dec), 6 May, **10 May**, (31 May)
7	Layered erosion	16 Nov, 9 Dec (Grünloch) 15 Nov, 17 Nov (Seekopfalm)
8	Cold-air-pool window	22 Oct, 2 Nov, 9 Nov, 12 Nov, 14 Nov, 21 Nov, 7 Dec, 2 Feb, 7 Feb, 14 Feb, 15 Feb, 20 Feb, **6 Apr**, (2 May), (8 May), **9 May**, (21 May), 23 May
9	Multiday cold-air pool	(11 Nov), 17 Nov, 2 Dec, 3 Dec, (4 Dec), (9 Dec), (10 Dec), 15 Dec, 24 Dec, (28 Dec), (29 Dec), **4 Jan**, 5 Jan, **6 Jan**, **8 Jan**, **9 Jan**, **10 Jan**, **11 Jan**, (12 Jan), (14 Jan), **15 Jan**, **16 Jan**, (2 Feb)

highest-elevation weather station in the basin at Kleiner Hühnerkogel provided values of wind speed and virtual potential temperature that were representative of the well-mixed atmosphere at the top of a 10-m-deep erosion zone. Wind speeds and virtual temperatures at the base of the erosion zone were then estimated from measurements at the lower-altitude weather stations at the Lechner Saddle and the Grünloch base.

4. Cold-air-pool events

Examples of the major categories of observed nighttime cold-air-pool events are illustrated in Fig. 2 using time series data from the Grünloch floor (GL00D), the 16 temperature dataloggers on the northwest line (NW01–NW16), and the 15 temperature dataloggers on the southeast line (SE01–SE15). At locations where more than one temperature logger was operated, a supplemental suffix indicates whether the data from the upper (U) or lower (D) instrument were used. The examples are chosen from times of the year when all or most of the temperature dataloggers of the selected lines and the automatic weather stations were above the snowpack, that is, mainly from late autumn or early spring. Table 2 provides a list of all of the dates of each of the cold-air-pool-event categories. There were occasional instances for which more than one event was noted on a single night.

a. Undisturbed evolution

The dataset contained nine nights with absolutely undisturbed cold-air pools and an additional six nights with nearly undisturbed conditions. These events were characterized by rates of cooling that were very strong at the lowest altitudes of the sinkhole in the first 3 h following local sunset [1700 central European time (CET) in late October], but the cooling rates decreased with altitude. Cooling rates tapered off gradually with time through the remainder of the night at the lower elevations of the Grünloch while temperatures remained nearly constant at the upper altitudes. Although we consider these 15 events to be undisturbed, there are frequently short-term temperature oscillations superimposed on the cooling curves at individual sites that are thought to represent oscillations in the slope flows (e.g., Doran and Horst 1981).

Perfectly undisturbed cold-air pools occurred only on nights with anticyclonic weather and light background winds. On these nights, winds at the Kleiner Hühnerkogel summit, 1 km southwest of the sinkhole, were typically 1–2 m s^{-1}, with maximum winds below 4–5 m s^{-1}. Winds at the weather station on the sinkhole floor became nearly calm after the cold-air pool formed, although speeds intermittently reached 0.1–0.3 m s^{-1}. Humidity varied between 20% and 90% at the Kleiner Hühnerkogel summit during these events, but the humidity level seemed to have little influence on the cold-air-pool buildup, as long as clouds were not present.

From 11 to 19 October 2001 a pronounced high pressure zone dominated over central and western Europe. Skies over Austria were mostly clear, with some increasingly persistent fog over the lowlands and valleys toward the end of this period. On 18–19 October (Fig. 2a) an inversion

of about 20°C developed over the 142-m altitude difference between the lowest- and highest-altitude dataloggers, with sharp temperature decreases starting as early as 1500–1600 CET. From 1900 to 0030 CET, winds at Kleiner Hühnerkogel increased temporarily from 1–2 to 3–5 m s^{-1} but still were not able to degrade the inversion. Relative humidity ranged between 40% and 60% at the mountain top and remained constant at the sinkhole bottom (95%). A very rapid warming occurred at all stations in the 2.5 h following local sunrise at the sinkhole floor, and the temperature profiles overturned (i.e., temperature decreased with height) after the inversion was destroyed by 1000–1100 CET. Mechanisms leading to the postsunrise breakup of a valley or basin inversion have already been described in the literature (Whiteman et al. 2004c). The 3 June 2003 breakup of a Grünloch inversion followed a pattern of inversion destruction (pattern 2) that was originally seen in Colorado valleys (Whiteman 1982).

b. Late buildup

Fourteen late-inversion-buildup events were observed during the observational period. These late events typically occurred when clouds dissipated and/or winds weakened in the sinkhole—for example, after the nighttime passage of fronts. In these events, the temporal evolution of the cold-air pool was similar to the undisturbed buildup, except for the late start.

On 16 November 2001 the Grünloch region was located on the eastern flank of a high pressure system centered over Ireland in a northwesterly flow. A weak warm front was embedded in this flow, causing midlevel clouds in the region. During the day the high pressure zone expanded slowly over central Europe. After a mostly cloudy day, the 5.5-km-distant synoptic (SYNOP) station Lunz am See (615 m MSL) reported clear sky, a snow cover of 17 cm, and −6.8°C at 1900 CET. The onset of the 16–17 November 2001 event (Fig. 2b) in the basin began around 0030 CET. Before that time, gusty winds with speeds up to 3 m s^{-1} occurred at the basin floor. The cold-air pool began to form when the winds on the summit of the Kleiner Hühnerkogel decreased from 4 to 1 m s^{-1}. At the same time, relative humidity at the summit started to decrease from 95% at 0030 CET to approximately 20% at 0830 CET. The minimum temperature at the basin floor, −22.1°C, occurred at 0830 CET. We assume that the increasing wind speeds at Kleiner Hühnerkogel of up to 10 m s^{-1} were the major mechanism for removing the cold-air pool by turbulent mixing with upper-layer air in the morning hours. A snowpack of about 20 cm (Steinacker et al. 2007) increased the albedo in the basin, which reduced the heating of the surface layer and avoided the buildup of a convective boundary layer. The role of upslope winds on the destruction of the cold-air pool is difficult to estimate without additional data. On the one hand, heating of the snow-covered slopes is reduced, minimizing upslope winds. On the other hand, snow-free trees on the slopes may absorb much of the incoming shortwave radiation, increasing the upslope winds.

c. Early breakup

Early breakup of cold-air pools requires a strong disturbance to an existing nighttime cold-air pool. Twelve such events occurred during the observational period. Frontal passages and foehn onsets are the two most common reasons for early inversion breakup. To remove a cold-air pool successfully, wind speeds typically had to exceed 5 m s^{-1} at the weather station on the Kleiner Hühnerkogel summit depending on the prevailing stability. This wind speed threshold is slightly lower than the 7–9 m s^{-1} found by Rakovec et al. (2002) for the much larger Ljubljana basin. Zhong et al. (2003), in their semitheoretical study, found that 7 m s^{-1} was the minimum wind speed threshold for winds aloft to start turbulent erosion for a much deeper erosion layer of 50 m.

On 18–19 May 2002 a weak cold front passed the Grünloch region around 0200 CET, marked by increasing wind speeds, a drop in equivalent potential temperature at the Kleiner Hühnerkogel summit, a pressure rise, and a change in wind direction. Cold-air advection above the inversion reduced the stability and allowed the moderate wind speeds to erode the cold-air pool. Figure 3a shows R_B for this event. At 0130 CET, R_B between Kleiner Hühnerkogel and Lechner Saddle dropped below 0.25 and turbulent erosion of the basin inversion began. One hour later, R_B between Kleiner Hühnerkogel and Grünloch floor also reached the 0.25 limit, and by 0330 CET the cold-air pool was completely removed. Moreover, higher values of humidity at Kleiner Hühnerkogel (up to almost 100%) came with the front, suggesting an increase in cloud coverage and a lowering of cloud base. This would lead to increased back-radiation that would contribute to cold-air-pool removal.

d. Mixing events

Strong, gusty winds frequently caused disturbances in the cold-air-pool buildup cycle. When winds above the inversion became strong, turbulent eddies mixed down the warmer air at the top of the inversion, causing temperatures to rise in the basin below. Strong, gusty winds often interacted with the ridgeline topography to produce energetic eddies that were especially effective in vertical mixing of air in the upper basin. Twenty-three such events were observed during the observational period. The rate of mixing is assumed to depend on

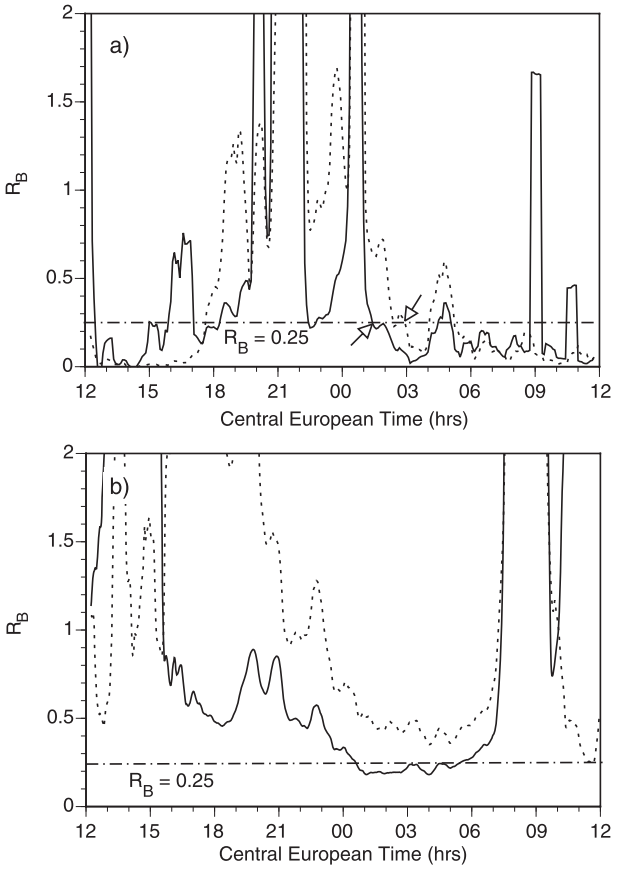

FIG. 3. Bulk Richardson number R_B (30-min running mean; Δz = 10 m) for the (a) 18–19 May 2002 early-breakup event and (b) 19–20 Oct 2001 upper-disturbance event. For a detailed description of how R_B was estimated, see section 3. Solid lines are values calculated from W3 and W2; dotted lines are values calculated from W3 and W1. Values of R_B of >2 have been omitted.

several parameters: 1) the vertical shear of the horizontal winds, 2) the sizes and energies of the eddies generated by this shear, 3) the interactions with the surrounding higher topography, and 4) the stability within the cold-air pool. Turbulent processes drive the basin atmosphere toward a neutral temperature structure of $-dT/dz = 9.8$°C km^{-1}. Increases in cloudiness, on the other hand, contribute to the destabilization of the basin atmosphere by driving the basin atmosphere toward isothermal stratification as a radiative equilibrium is established between the cloud base and the underlying topography of the basin.

Ahead of a trough over western Europe a southwesterly flow became established on the night of 30 April–1 May 2002 over the Alps. This caused a short foehn episode in the Grünloch area. At 2000 CET 30 April wind speed increased from 2 to 7 m s^{-1}, with gusts up to 10 m s^{-1} at the weather station on the Kleiner Hühnerkogel summit. Wind directions were southerly. Within the next 12 h, relative humidity decreased from about 65% to 30% and potential temperature increased by 10°C at this station. These increasing winds were strong enough to ''mix out'' the incipient or weakly developed cold-air pool at 2100 CET, the time period with the strongest gusts (Fig. 2d). After that, the winds decreased again and the cold-air-pool buildup began anew. A secondary wind speed maximum later in the night of 5–6 m s^{-1} could not erode the cold-air pool again since the warm-air advection above increased the stability.

e. Upper disturbance

Disturbances in the upper part of the cold-air pool were related to winds above the inversion, as was shown for the ''mixing'' case. The ''upper disturbance'' cases differ from the mixing-event cases in that winds above the cold-air pool are steady but insufficiently strong or turbulent enough to remove the cold-air pool. They simply produce a warming and/or a decrease in the temperature gradient in the still-stable upper part of the cold-air pool. Twenty-three such events were observed in the period of record.

The synoptic situation on 19–20 October 2001 was characterized by a ridge over central Europe flanked by two large cyclones—one over the eastern Atlantic Ocean and one over western Russia (see also the synoptic description in section 4a). A short-wave trough made it around the ridge, however, and the southernmost tip reached the Grünloch region on the night of 19–20 October. At 2000 CET wind speeds started to increase from 2 to 5 m s^{-1} with gusts up to 7 m s^{-1} at 0400 CET at Kleiner Hühnerkogel. Relative humidity stayed below 60% for the whole event. Despite the fact that wind speeds exceeded 5 m s^{-1}, the cold-air pool was not eroded completely. Only the stability in the upper cold-air pool was reduced (Fig. 2e), especially in the layer between 50 and 80 m above the basin floor, with a slow recovery between 0200 and 0700 CET. This is supported by the estimation of R_B for this event (Fig. 3b). At 0030 CET R_B between Kleiner Hühnerkogel and Lechner Saddle dropped below 0.25 and turbulent erosion of the basin inversion began. In contrast with the early breakup event (Fig. 3a), however, R_B between Kleiner Hühnerkogel and the Grünloch floor never reached the 0.25 limit and the cold-air pool prevailed. Figure 4 decomposes R_B into its main components, stability and wind shear. Although wind speeds were comparable, it was gustier in the early-breakup case (Fig. 4a). In the upper-disturbance case (Fig. 4b), the stability as indicated by the virtual potential temperature difference between the Kleiner Hühnerkogel and the basin floor was much stronger.

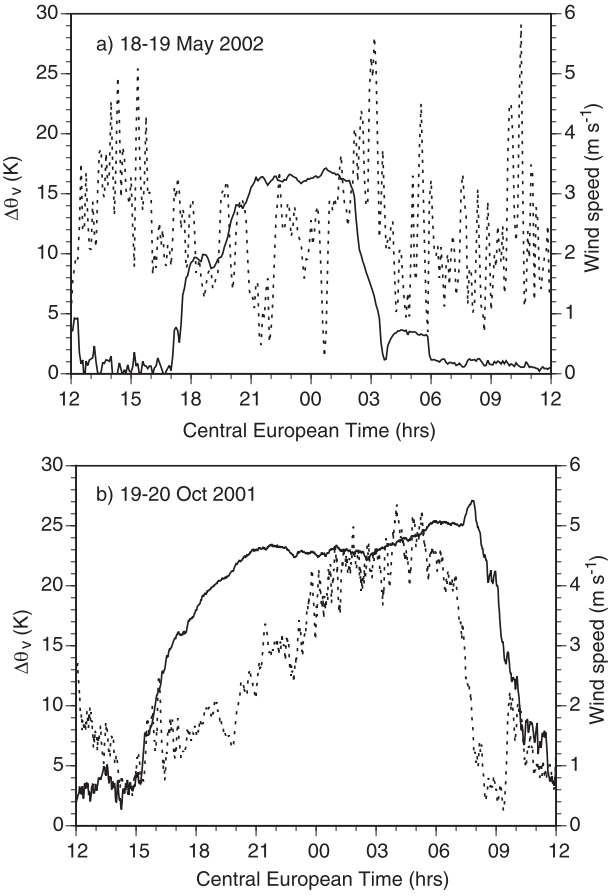

FIG. 4. Wind speeds (10-min mean) and stability in terms of difference of θ_v between the Kleiner Hühnerkogel and the Grünloch basin station for the (a) early-breakup case (18–19 May 2002) and (b) upper-disturbance case (19–20 Oct 2001); see also Fig. 2. Solid lines are $\Delta\theta_v$; dotted lines are wind speed.

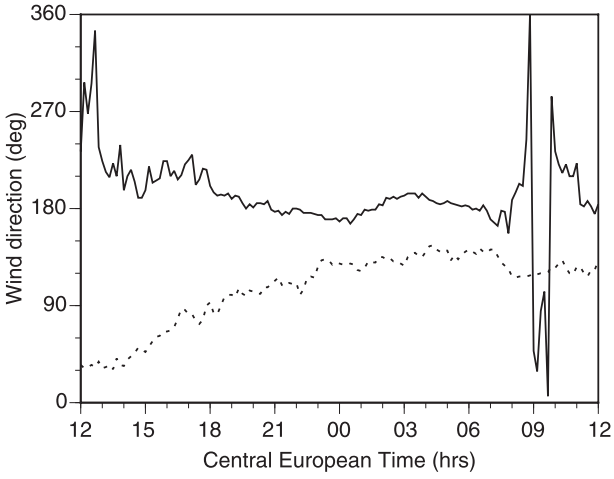

FIG. 5. Wind directions at the Kleiner Hühnerkogel station for the mixing-event case (Fig. 2d; solid line) and for the layered-erosion case (Fig. 2g; dotted line).

f. Lower disturbance

Ten cold-air-pool events produced a temporary temperature rise that was confined to the lowest stations in the basin. In contrast with short-term temperature fluctuations, the lower disturbance is greatest at the basin floor and decreases with elevation. Further, their time scale is on the order of hours in contrast with the 5–15-min periodicity of short-term temperature fluctuations. These lower cold-air-pool disturbances are still not well understood. Perhaps these temperature anomalies of order 1–2 K are caused by the back-radiation from clouds that pass over the experimental area or from cold-pool disturbances caused by clouds that form within the basin. As an alternative, the disturbances could be caused by any phenomenon that increases turbulence (and the consequent downward mixing of warmer air from aloft) on the slopes in the lower basin while being absent from the upper basin.

The governing weather system on the night of 1–2 December was an anticyclone located over central Russia with a core pressure of more than 1055 hPa extending over the eastern Alps. The prevailing weather phenomena in the Grünloch region for weather systems of this type are weak winds, fog and low stratus in valleys and lowlands, and clear skies in the mountain areas. On that night, a low-level disturbance occurred (Fig. 2f) at the five lowermost sites on the basin floor, starting at 1900 and lasting until 1930 CET. Undisturbed nighttime cooling was reestablished following this event. The nearby station at the Kleiner Hühnerkogel summit reported almost calm conditions, with relative humidity varying between 50% and 70%. Calm winds were observed in the Grünloch basin except during the period of 1850–1920 CET when light winds with ''gusts'' of up to 1 m s^{-1} from northeasterly directions occurred. Relative humidity in the basin did not exceed 82% during the entire night.

g. Layered erosion

Turbulent erosion of a cold-air pool is a slow removal process in which the upper part of the cold-air pool is removed layer by layer by turbulence generated at the interface between the cold-air pool and the atmosphere above by strong winds. Previous research on this phenomenon suggests that the winds above the inversion must increase in speed to continue the removal process (Petkovšek 1992; Rakovec et al. 2002; Zhong et al. 2003). Two cases of turbulent erosion were observed at the Grünloch, neither of which completely destroyed the cold-air pools. Two other cases were observed in the smaller adjacent Seekopfalm sinkhole. One of them required

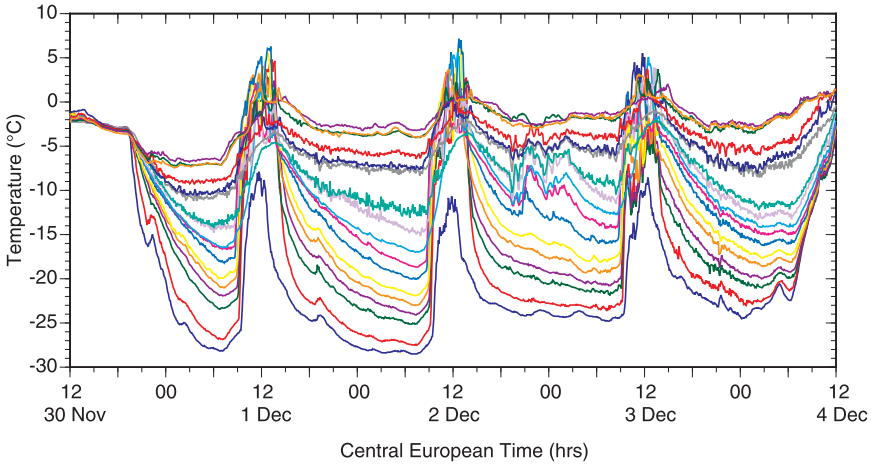

FIG. 6. Grünloch multiday cold-air pool, 30 Nov–4 Dec 2001. The northwest line of temperature dataloggers is used.

3.5 h to destroy a 20°C temperature inversion in the 26-m-deep sinkhole (see Steinacker et al. 2007).

An upper-level cyclone passed south of the Grünloch in a northeasterly-to-southeasterly direction on the night of 9–10 December 2001. With this cyclone track, wind directions shifted from northeasterly through easterly to southeasterly at Kleiner Hühnerkogel. As the topographic map of Fig. 1 shows, there is a wide gap on the southeast edge of the basin that makes southeasterly winds the preferred wind direction for the layer-by-layer removal of the cold-air pool. At SE05, which is located 26 m above the basin floor, a first attempt at cold-air-pool removal occurred at 1740 CET (Fig. 2g). Wind speeds did not exceed 4 m s^{-1} at that time, however. Around 2140 CET, wind speeds increased to 6–8 m s^{-1} with wind directions from 120° to 130°, and the erosion process started anew. As Fig. 2g shows, 2 h were needed to remove an 11-m-thick layer (layer thickness between SE05 and SE03). Between 0100 and 0300 CET, wind speeds decreased slightly and the removal process stopped. Later on, a new period of high wind speeds up to 11 m s^{-1} at the Kleiner Hühnerkogel station removed the next layer, but, since the wind speed did not increase further, the last 5–8 m of the cold-air pool could not be eroded.

One might expect the response of the cold-air pool to background winds to depend very much on the sheltering of the pool provided by the surrounding higher terrain. Because the height and character of the surrounding terrain vary for winds aloft that approach the sinkhole from different directions, the response of the cold-air pool might differ significantly for different wind directions. Large eddies shed from the surrounding ridgetops may significantly perturb the entire stable boundary layer in the sinkhole, whereas smaller eddies are responsible for a slow erosion of the inversion top. This speculation is supported by comparing the wind directions of the mixing event in Fig. 2d and the layered erosion event in Fig. 2g, as shown in Fig. 5. For the mixing event, the dominant wind directions are between 180° and 190°. This means that winds had to pass the higher and sharp ridgeline south of the basin (see Fig. 1), creating much turbulence. For the layered-erosion events, the preferred wind directions are from 100° to 110°. From these directions, the flow passes a broad saddle (see Fig. 1), creating turbulence on a smaller scale than for the previous type.

h. Cold-air-pool window

Even on nonideal nights with strong winds or clouds, short-lived inversion-buildup episodes were often observed. A cloud gap or a short calm period of 30 min or less is enough to initiate these episodes. Eighteen events of this type were recorded during the experimental period. Because of the adverse weather situation, these cold-air pools have a short lifetime of up to 1 or 2 h and the development of a stronger, longer-lasting pool is not possible. Depending on the duration of the event, the depth of the cold-air pool varies from several meters to the whole basin depth. The advection of a cloud gap across the Grünloch sinkhole or a sudden lull in the background winds causes the temperature profiles to evolve rapidly, providing an indication of the basin atmosphere's response to external influences (De Wekker and Whiteman 2006).

On 12–13 November 2001 (Fig. 2h), a 20-min-long cold-air-pool window caused temperatures at the ground to fall by 3°C. The synoptic charts show the experimental area to be under the decreasing influence of an occlusion from a cyclone located over the western Mediterranean Sea and show a new approaching cold front from northerly directions. The thermal infrared image

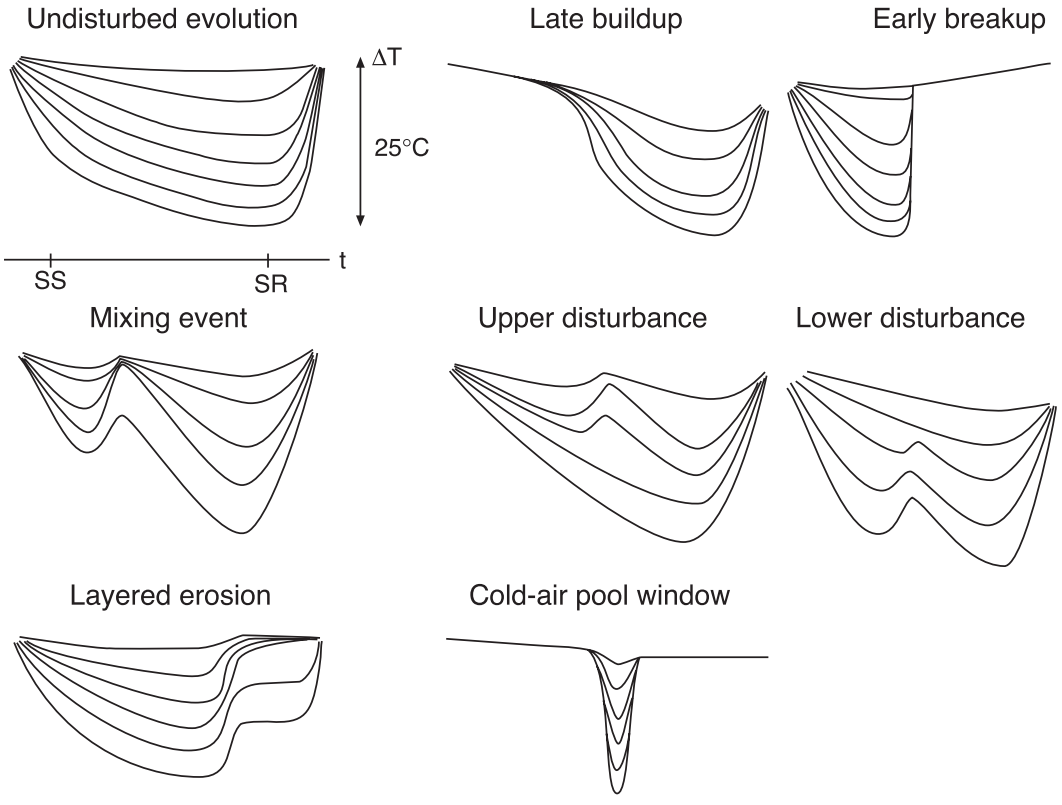

FIG. 7. Summary schematic diagram illustrating the different classifications of cold-air-pool events in the Grünloch basin. The plots represent temperature times series patterns from temperature measurements at different altitudes on the sidewalls. The plots illustrate single-night events. An additional type of event, not illustrated here, is the multiday cold-air pool.

of Meteosat (not shown) indicates a gap in the cloud cover for 0700 CET in the area around the Grünloch basin. Because data were not available from any of the weather stations for this case, we cannot determine whether a wind speed lull contributed to this event.

i. Other events

There were five nights (19 October, 20 October, 15 November, 9 December, and 6 May) when upper and lower disturbances occurred at the same time. Synchronous upper and lower disturbances were not considered to be a separate event category. In some instances, these contemporaneous disturbances appeared to represent vertical displacements of cold-air-pool air, in which the largest temperature changes occurred at elevations having the greatest vertical temperature gradient. Temperature changes ΔT are greatest for the same vertical displacement Δz in high-stability regions, following the relation $\Delta T = (\gamma - \Gamma_d)\Delta z$, where γ is the environmental lapse rate and Γ_d is the dry adiabatic lapse rate.

Twenty-three multiday cold-air-pool events occurred during the experimental period. On midwinter days, some parts of the sinkhole remain in the shadow of the surrounding ridgelines and receive no direct solar radiation, so that it is difficult for the cold-air pool to be completely destroyed by daytime heating, especially when snow cover is on the ground and trees or when clouds limit the incoming shortwave radiation. Often, the cold-air pool persists as a shallow remnant of the deeper nighttime cold-air pool. The multiday cold-air pool of 30 November–4 December 2001 is plotted in Fig. 6. This event began after a fresh snowfall on 30 November, and the largest cold-air-pool temperature deficit occurred on the first full night following the snowfall. Despite a strong daily heating cycle that peaked at around noon on each of the days of this event, relatively cold temperatures remained at the lowest site on the basin floor, indicating that the cold-air pool remained intact, although shallow.

A variety of short-term or localized subevents occurred in connection with the major events. An example, already mentioned, is the short-term temperature oscillations associated with slope flows, turbulence events, or changes in cloud cover. Short-term changes in stability that occur intermittently at different heights can be seen in the time series of Figs. 2a–f.

5. Summary and conclusions

The range of different types of cold-air-pool events in the Grünloch basin that have been illustrated with actual temperature time series data in Fig. 2 are summarized in schematic fashion in Fig. 7. The first event, an undisturbed cold-air-pool evolution, can be contrasted with the other types of events in this figure. The plots illustrate the time series of temperature observations made from different heights on the basin sidewall for the individual events. The coldest temperature curve in each of the plots is from the basin floor, and the warmest temperature curve is from the highest sidewall elevation. A time scale showing the approximate times of astronomical sunrise and sunset that is marked on the undisturbed-evolution plot is applicable to all other plots. The temperature scale, however, is applicable only to the first plot, and the others are not to scale.

Analysis of temperature time series from lines of temperature sensors running up the northwest and southeast sidewalls of the Grünloch sinkhole or basin in the eastern Alps has led to a categorization of meteorological events that modify the normal development of cold-air pools. A schematic diagram was developed to illustrate these different types of events. The events include undisturbed cold-air-pool evolution, late inversion buildups, early inversion breakups, cold-air-pool mix-out events, modification of the cold-air pool as a result of disturbances in the upper and lower basin atmosphere, layered erosion at the cold-air-pool top, cold-air-pool modifications caused by the sudden onset or cessation of overcasts or lulls in background winds, and multiday cold-air pools. The causes of the events were investigated by reference to synoptic charts and to data from three automatic weather stations in the sinkhole and its immediate surroundings. The number of events occurring in the 17 October 2001–4 June 2002 period of record was presented in tables. The results show that undisturbed cold-air-pool events are actually unusual and that the cold-air pools in this climatic setting are often modified by cloudy and windy conditions.

Acknowledgments. We thank P. Kupelwieser for providing access to the experimental area. We also thank the organizers and participants of the 2001–02 Grünloch experiments and, especially, students from the University of Vienna for their many contributions to the field program. CDW acknowledges research support from U.S. National Science Foundation Grants ATM-0444205 and ATM-0521776 and from the U.S. Department of Energy (DOE) under the Atmospheric Sciences Program of the Office of Biological and Environmental Research. Portions of this research were conducted at Pacific Northwest National Laboratory (PNNL), which is operated for the DOE by Battelle Memorial Institute. Two authors (SE and BP) thank the University of Vienna, the state of Lower Austria, the DOE, and PNNL for fellowships served at PNNL in 2002 and 2003. Thanks are also given to the Department of Meteorology and Geophysics of the University of Vienna for partial funding of the experiment.

REFERENCES

Aigner, S., 1952: Die Temperaturminima im Gstettnerboden bei Lunz am See, Niederösterreich (The minimum temperatures in the Gstettner basin near Lunz, Lower Austria). *Wetter Leben* (Special Issue 1), 34–37.

Billings, B. J., V. Grubišić, and R. D. Borys, 2006: Maintenance of a mountain valley cold pool: A numerical study. *Mon. Wea. Rev.,* **134,** 2266–2278.

Clements, C. B., C. D. Whiteman, and J. D. Horel, 2003: Cold-air-pool structure and evolution in a mountain basin: Peter Sinks, Utah. *J. Appl. Meteor.,* **42,** 752–768.

De Wekker, S. F. J., and C. D. Whiteman, 2006: On the time scale of nocturnal boundary layer cooling in valleys and basins and over plains. *J. Appl. Meteor.,* **45,** 813–820.

Doran, J. C., and T. W. Horst, 1981: Velocity and temperature oscillations in drainage winds. *J. Appl. Meteor.,* **20,** 361–364.

Fritts, D. C., D. Goldstein, and T. Lund, 2010: High-resolution numerical studies of stable boundary layer flows in a closed basin: Evolution of steady and oscillatory flows in an axisymmetric Arizona Meteor Crater. *J. Geophys. Res.,* **115,** D18109, doi:10.1029/2009JD013359.

Geiger, R., 1965: *The Climate near the Ground*. Harvard University Press, 482 pp.

Glickman, T., Ed., 2000: *Glossary of Meteorology*. 2nd ed. Amer. Meteor. Soc., 855 pp.

Kunze, E., A. J. Williams III, and M. G. Briscoe, 1990: Observations of shear and vertical stability from a neutrally buoyant float. *J. Geophys. Res.,* **95,** 18 127–18 142.

Petkovšek, Z., 1992: Turbulent dissipation of cold air lake in a basin. *Meteor. Atmos. Phys.,* **47,** 237–245.

Pospichal, B., 2004: Struktur und Auflösung von Temperaturinversionen in Dolinen am Beispiel Grünloch (Structure and evolution of temperature inversions in dolines, exemplified by the Grünloch). Diploma thesis, Dept. of Meteorology and Geophysics, University of Vienna, 68 pp.

Rakovec, J., J. Merše, S. Jernej, and B. Paradiž, 2002: Turbulent dissipation of the cold-air pool in a basin: Comparison of observed and simulated development. *Meteor. Atmos. Phys.,* **79,** 195–213.

Steinacker, R., and Coauthors, 2007: A sinkhole field experiment in the eastern Alps. *Bull. Amer. Meteor. Soc.,* **88,** 701–716.

Vrhovec, T., and A. Hrabar, 1996: Numerical simulations of dissipation of dry temperature inversions in basins. *Geofizika,* **13,** 81–96.

Whiteman, C. D., 1982: Breakup of temperature inversions in deep mountain valleys: Part I. Observations. *J. Appl. Meteor.,* **21,** 270–289.

——, 1990: Observations of thermally developed wind systems in mountainous terrain. *Atmospheric Processes over Complex Terrain, Meteor. Monogr.,* No. 45., Amer. Meteor. Soc., 5–42.

——, and T. B. McKee, 1982: Breakup of temperature inversions in deep mountain valleys: Part II. Thermodynamic model. *J. Appl. Meteor.,* **21,** 290–302.

——, J. M. Hubbe, and W. J. Shaw, 2000: Evaluation of an inexpensive temperature data logger for meteorological applications. *J. Atmos. Oceanic Technol.,* **17,** 77–81.

——, S. Zhong, W. J. Shaw, J. M. Hubbe, X. Bian, and J. Mittelstadt, 2001: Cold pools in the Columbia basin. *Wea. Forecasting,* **16,** 432–447.

——, S. Eisenbach, B. Pospichal, and R. Steinacker, 2004a: Comparison of vertical soundings and sidewall air temperature measurements in a small Alpine basin. *J. Appl. Meteor.,* **43,** 1635–1647.

——, T. Haiden, B. Pospichal, S. Eisenbach, and R. Steinacker, 2004b: Minimum temperatures, diurnal temperature ranges, and temperature inversions in limestone sinkholes of different size and shape. *J. Appl. Meteor.,* **43,** 1224–1236.

——, B. Pospichal, S. Eisenbach, P. Weihs, C. B. Clements, R. Steinacker, E. Mursch-Radlgruber, and M. Dorninger, 2004c: Inversion breakup in small Rocky Mountain and Alpine basins. *J. Appl. Meteor.,* **43,** 1069–1082.

——, S. F. J. De Wekker, and T. Haiden, 2007: Effect of dewfall and frostfall on nighttime cooling in a small, closed basin. *J. Appl. Meteor.,* **46,** 3–13.

——, and Coauthors, 2008: METCRAX 2006: Meteorological experiments in Arizona's Meteor Crater. *Bull. Amer. Meteor. Soc.,* **89,** 1665–1680.

Yao, W., and S. Zhong, 2009: Nocturnal temperature inversions in a small, enclosed basin and their relationship to ambient atmospheric conditions. *Meteor. Atmos. Phys.,* **103,** 195–210.

Zängl, G., 2002: An improved method for computing horizontal diffusion in a sigma-coordinate model and its application to simulations over mountainous topography. *Mon. Wea. Rev.,* **130,** 1423–1432.

——, 2005: Formation of extreme cold-air pools in elevated sinkholes: An idealized numerical process study. *Mon. Wea. Rev.,* **133,** 925–941.

Zhong, S., C. D. Whiteman, X. Bian, W. J. Shaw, and J. M. Hubbe, 2001: Meteorological processes affecting the evolution of a wintertime cold air pool in the Columbia basin. *Mon. Wea. Rev.,* **129,** 2600–2613.

——, X. Bian, and C. D. Whiteman, 2003: Time scale for cold-air pool breakup by turbulent erosion. *Meteor. Z.,* **12,** 229–233.